Thin Calorimetry for Cosmic-Ray Studies Outside the Earth's Atmosphere

Richard WIGMANS

Department of Physics, Texas Tech University, Lubbock TX 79409-1051, USA

(wigmans@ttu.edu)

Abstract

Cosmic ray experiments outside the Earth's atmosphere are subject to severe restrictions on the mass of the instruments. Therefore, it is important that the experimental information that can be obtained per unit detector mass is maximized. In this paper, tests are described of a thin (1.4 $\lambda_{\rm int}$ deep) hadron calorimeter that was designed with this goal in mind. This detector was equipped with two independent active media, which provided complementary information on the showering hadrons. It is shown that by combining the information from these media it was possible to reduce the effects of the dominant leakage fluctuations on the calorimeter performance.

1 Introduction

In recent years, there has been an increased interest in the use of calorimetric techniques in cosmic-ray experiments outside the Earth's atmosphere. Calorimeters have been applied in experiments carried out in stratospheric balloon flights, in satellites and in the Space Shuttle. Several experiments are currently being planned for the International Space Station. These experiments focus on measuring features of the cosmic rays that are inaccessible with Earth-bound detectors, *e.g.*, the antiproton content, the chemical and isotopic composition and the high-energy electron and photon spectra.

One common aspect of all these experiments is the severe restriction on the mass of the detectors. For calorimeters, this restriction poses a new challenge: *How can one maximize the calorimetric information per unit detector mass?*

When high-energy hadrons develop showers in a 1–2 $\lambda_{\rm int}$ deep calorimeter, the response function is completely determined by leakage fluctuations. These fluctuations are very likely correlated with the fraction of energy spent on π^0 production inside the detector. In general, π^0s produced in the first nuclear interaction develop electromagnetic (em) showers that are contained in the detector, while charged pions typically escape. Therefore, events in which a large fraction of the initial energy is converted into π^0s in the first interaction will exhibit little leakage (a large detector signal), while events in which a small fraction of the energy has been transferred to π^0s will be characterized by large leakage (small detector signals).

It has been demonstrated experimentally that calorimeters using quartz fibers as active material are almost exclusively sensitive to the π^0 component of hadron showers [1]. This is because most of the energy in the non-em component is deposited by non-relativistic shower particles, which do not emit Čerenkov light, the source of experimental information in this type of detector [2].

We have used this feature in an attempt to get a handle on the (leakage) fluctuations that dominate the performance of very thin hadron calorimeters, and thus improve this performance. A dual-readout calorimeter that measures both the ionization losses (dE/dx) and the production of Čerenkov light might distinguish between events with relatively small and large shower leakage, since the ratio of the two signals would be different in these two cases: A relatively large Čerenkov signal would indicate relatively little shower leakage, while a small Čerenkov signal (compared to the dE/dx signal) would suggest that a large fraction of the shower energy escaped from the detector.

A group at TTU has built and tested such a calorimeter, in the framework of prototype studies for the Advanced Cosmic Composition Experiment at the Space Station (ACCESS). In this paper, some results of beam tests of this calorimeter are presented.

2 The detector

The calorimeter consisted of 39 lead plates (with a thickness of 6.4 mm each, for a total depth of 1.4 $\lambda_{\rm int}$ or 46 X_0). These plates were interleaved with alternating ribbons of scintillating and quartz fibers, providing x, y-readout and an effective tower structure for particles entering perpendicular to the absorber plates, for both types of light (Figure 1).

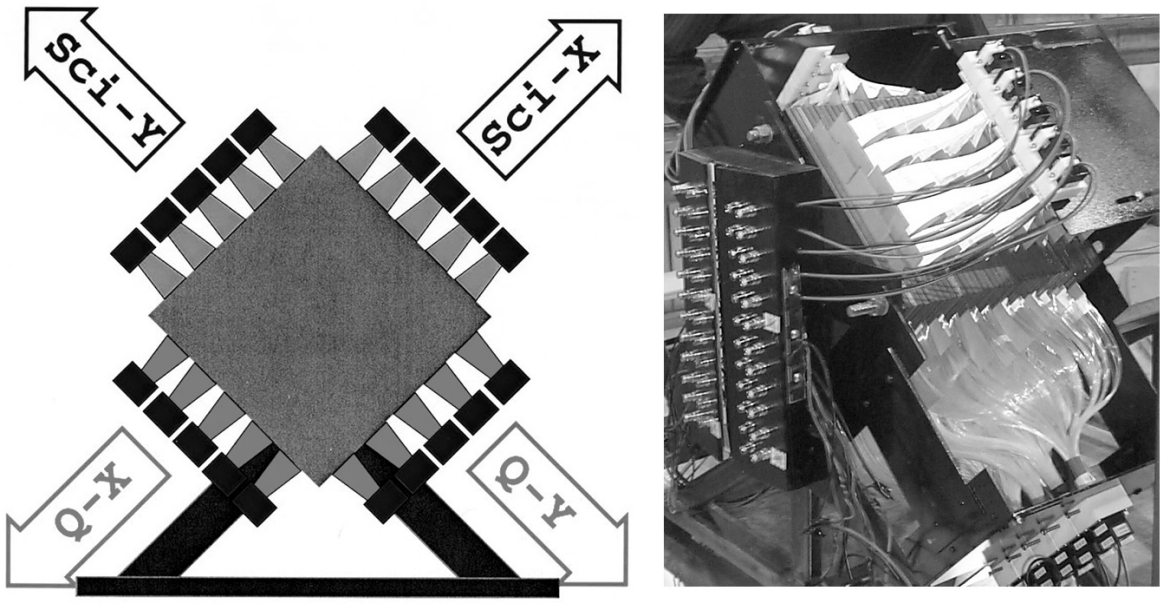

Figure 1: Schematic layout of the dual-readout calorimeter (left) and a photograph showing part of the actual instrument (right). See text for details.

The scintillating fibers[1] were 500 μm thick and had a numerical aperture of 0.72. The quartz fibers[2] were 270 μm thick and their numerical aperture was 0.40. The showering particles generated scintillation light in the plastic fibers and Čerenkov light in the quartz fibers. Photons emitted within the numerical aperture of the fibers were captured and transported through internal reflection to the fiber ends, where they were converted into photoelectrons in the photocathode of a photomultiplier tube (PMT)[3].

The fiber ribbons were inserted between the absorber plates according to the following scheme. Plate 1 was followed by a layer of quartz fibers oriented in the x direction (Q_x), plate 2 by a layer of quartz fibers oriented in the y direction (Q_y). The first layer of scintillating fibers (S_x, oriented in the x direction) was located behind absorber plate 3. Plates 4,5 and 6 were followed by layers of the types Q_x, Q_y and S_y, respectively. This pattern for the first six sampling layers was repeated subsequently.

Each fiber layer consisted of five 40 mm wide ribbons. The instrumented detector volume thus comprised a surface area of 20×20 cm^2 that extended over a depth of 28 cm. The five ribbons were read out separately, combined with the corresponding ribbons located at other depths in the structure. For example, the Q_x ribbons located behind absorber layers #1,4,7,10,13,16,19,22,25,28,31,34 and 37 were ganged together in five bunches read out by five PMTs. Also the S_x, S_y and Q_y ribbons were read out by five PMTs each, giving a total of 20 electronic channels.

[1] SCSN-81, a polystyrene-based product manufactured by Kuraray Inc., Japan
[2] Manufactured by Fiberguide Industries, USA
[3] Hamamatsu R5900U, 10-stage

Because of the way the signals were read out, the calorimeter had a tower structure for particles entering it perpendicular to its front surface. In total, there were 25 towers, each with a cross section of 4×4 cm^2, both for the scintillating-fiber and the quartz-fiber signal readout.

This detector was tested in the H2 beam line of the SPS at CERN. It was mounted on a platform that could be moved vertically and laterally, so that the center of each tower could be moved into the beam, as needed for calibration purposes. Usually, the angle (θ) between the beam and the calorimeter's front face was 0°. However, we also performed some measurements in which the detector was rotated, at angles up to $\theta = 90^\circ$.

Upstream of the calorimeter, a trigger counter telescope was installed, which allowed a choice of the beam spot size for the recorded events. Downstream of the calorimeter, a large scintillation counter served as the "tail catcher". The hadron measurements were carried out with a $0.25\lambda_{\rm int}$ carbon target installed directly in front of the calorimeter. Scintillation counters placed directly upstream and downstream of this target made it possible to select events in which the beam particle had interacted in it. In the electron measurements, this target was replaced by a Preshower Detector, consisting of a 5 mm thick lead plate, followed by a scintillation counter. This device was very useful for eliminating hadron and muon contamination at very high energies.

All individual calorimeter cells were calibrated with 150 GeV electrons incident on the cell center.

3 Test results

3.1 *Electron measurements*

The detector was exposed to beams of electrons with energies of 50, 100, 150, 200, 250 and 300 GeV. The signal distributions of both the scintillating fibers and the quartz fibers were well described by Gaussian functions. The energy resolutions were measured to scale with $E^{1/2}$: $\sigma/E = 50\%/\sqrt{E}$ for the scintillating fibers, and $140\%/\sqrt{E}$ for the quartz fibers.

As was also found in tests of other quartz fiber calorimeters, the em resolution of the quartz component of our detector was completely dominated and determined by *photoelectron statistics* [1]. On average, em showers produced 0.5 photoelectrons per GeV deposited energy in the quartz fibers. For 200 GeV em showers, the signal was thus, on average, composed of 100 photoelectrons. Statistical fluctuations in that number led to an energy resolution of 10%. The em energy resolution measured with the scintillating fibers was dominated by *sampling fluctuations*, with a minor contribution from photoelectron statistics (the light yield was 20 p.e./GeV in this case).

The electron measurements also illustrated clearly the differences between the angular distributions of the scintillation light and the Čerenkov light produced by the shower particles (see Figure 2). The scintillation light is emitted isotropically when excited molecules in the scintillating fibers return to their ground state. On the other hand, the Čerenkov light is emitted in a cone with a 46° opening angle centered around the direction of the relativistic shower particles. As the angle of the incident electron beam was changed, the ratio of the signals observed in the x and y scintillating fibers was found to be essentially constant, whereas the ratio of the signals from the x and y quartz fibers strongly depended on the direction of the incoming particles. The latter effect was quantitatively in good agreement with the angular dependence of the signals from em showers measured in other quartz fiber calorimeters [3, 4].

The observed effect offers the opportunity to use the dual-readout calorimeter as a *goniometer*. A comparison of the total signals from the two perpendicular sets of quartz fibers provides information about the angle of incidence of the showering particles, a nice and unforeseen bonus.

3.2 *Hadron measurements*

Mainly as a result of the effects of incomplete shower containment, the signal distributions for high energy hadrons from this thin detector looked very different from the electron ones. Figure 3 shows some results for 375 GeV π^-. In

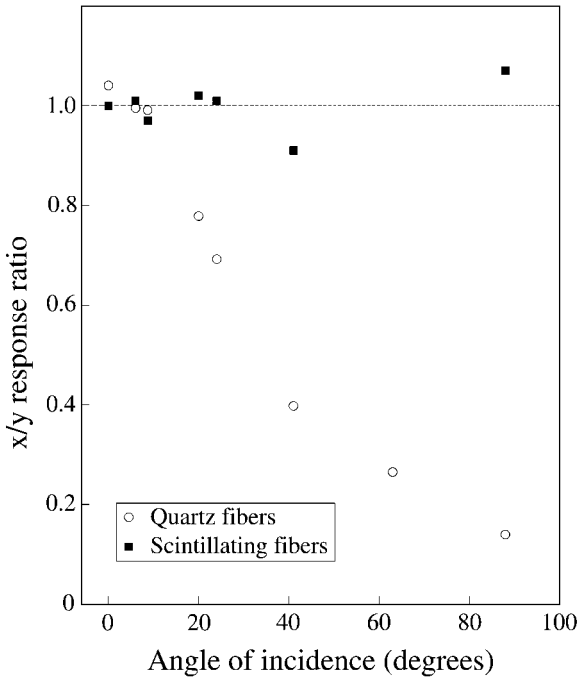

Figure 2: Ratio of the signals measured in fibers oriented in the x and y directions, as a function of the angle of incidence of the showering electrons (200 GeV). Results are shown separately for the quartz fibers and for the scintillating fibers.

Figure 3a, the signals recorded by the quartz fibers are plotted versus those from the scintillating fibers. The non-linear correlation between these signals indicates that they indeed measure different characteristics of the showers.

The scintillator signal distribution, *i.e.* the projection of the scatter plot on the horizontal axis, is shown in Figure 3b. The fact that this distribution is skewed to the low-energy side may be expected as a result of shower leakage. As we argued in Section 1, the relative strength of the quartz signal might be used as a handle on that leakage. For this reason, we investigated the merits of the *ratio of the signals from the quartz fibers and from the scintillating fibers*, Q/S, as an event-by-event measure of the shower leakage.

In Figure 3a, the signal ratio Q/S corresponds to the slope of a line through the bottom left corner of the scatter plot. The two lines drawn in this figure represent $Q/S = 1$ and $Q/S = 0.5$, respectively. On average, the Q/S ratio amounted to 0.77 at 375 GeV. The average value of the Q/S distribution was not very different for the other energies at which we performed our studies. The fact that the Q/S ratio is smaller than 1.0 indicates that a significant fraction, typically 20 - 25%, of the hadronic scintillator signal in this detector was caused by *non-relativistic* shower particles, predominantly protons released from nuclei in spallation processes, or recoiling from elastic neutron scattering in the plastic fibers.

In Figure 3c, the signal distribution is given for events with a small Q/S value ($Q/S < 0.45$). These events indeed populate the left-side tail of the calorimeter's response function (Figure 3b). This distribution is very different from the one obtained for events with Q/S ratios near the most probable value, shown in Figure 3d. The average values of the scintillator signal distributions in Figures 3c and 3d differ by about a factor of two.

These results demonstrate that events from the tails of the Q/S distribution correspond to events from the tails of the (dE/dx) response function. Therefore, we conclude that the ratio of the signals from the quartz and the scintillating fibers does indeed provide information on the energy containment and thus may be used to reduce the fluctuations that dominate the response function of this very thin calorimeter.

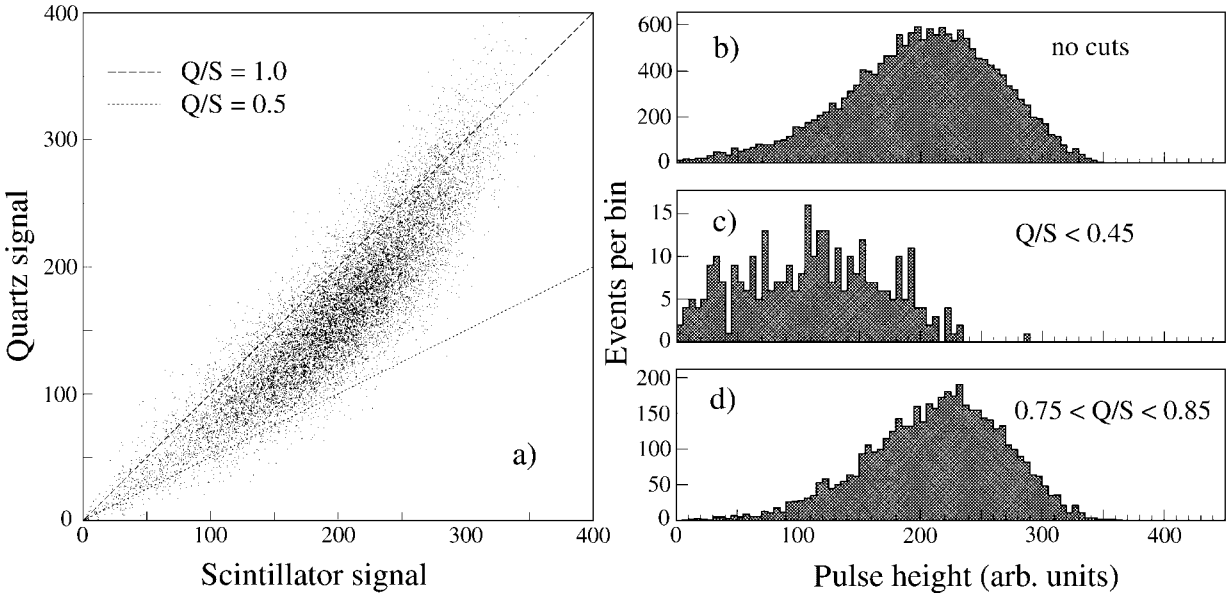

Figure 3: Test results for 375 GeV pions. Scatter plot of the signals recorded in the quartz fibers *vs.* those in the scintillating fibers (a). Signal distributions in the scintillating fibers, for all events (b) and for two subsets of events selected on the basis of their Q/S signal ratio (c, d).

We studied several methods of combining the signals from the two types of fibers and investigated their effects on the response function. The response function could also be improved by removing a small fraction of events with anomalously large or small Q/S values from the event sample. The improvement that could be achieved with such methods turned out to be primarily limited by the light yield of the quartz fibers. Fluctuations in the number of Čerenkov photoelectrons determined the width of the "banana" in Figure 3a and thus the selectivity of Q/S cuts. Therefore, the relative improvement in the energy resolution increased with the hadron energy. This is illustrated in Figure 4, which shows relative improvements in the energy resolution of up to $\sim 15\%$. These results were obtained by cutting 10% of the events from the tails of the Q/S distributions.

Figure 5 shows the fractional width of the distribution of the ratio of the signals from the quartz and the scintillating fibers, represented by the black dots, as a function of the energy of the incoming pions. This energy is plotted on a scale linear in $E^{-1/2}$, so that scaling with $\left[\sqrt{E}\right]^{-1}$ corresponds to a straight line through the bottom right corner of this plot. The experimental data, which cover an energy range of 150 – 375 GeV, are well described by such a line. This means that the width of the Q/S distribution in this energy range is completely determined by fluctuations governed by Poisson statistics, *i.e.* fluctuations in the number of photoelectrons produced by Čerenkov light from the quartz fibers.

As the energy is increased towards the region of interest for the cosmic ray studies, a further improvement of the energy resolution may thus be expected. This trend will continue until the point where factors other than the light yield in the quartz fibers start dominating the width of the Q/S distribution. Since the width of the Q/S distribution continued to improve over the entire energy range accessible in our tests, these experimental data did not allow us to estimate the ultimate improvement in energy resolution that is achievable with our method.

In an attempt to explore these limits, we rearranged the quartz fibers in the detector in such a way that the Čerenkov light from the showers was significantly increased. This was achieved by moving the quartz ribbons from the outermost layers of the detector to the central tower, thus effectively reducing the instrumented surface area from 20×20 cm^2 to 12×12 cm^2. The central tower was also equipped with PMTs with (UV transparent) quartz windows. These

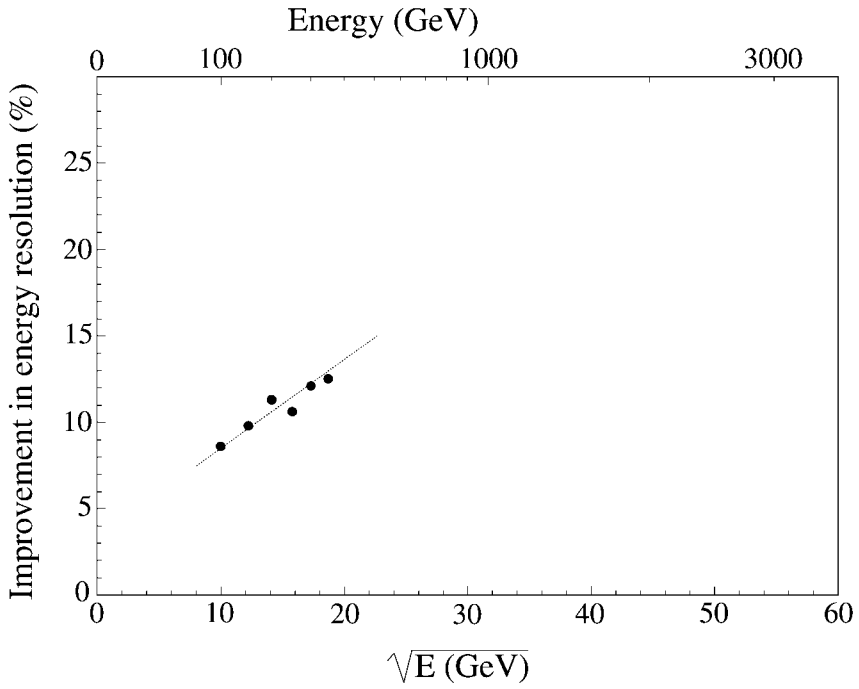

Figure 4: Improvement in the energy resolution for pions as a function of energy.

modifications resulted in an increase of the Čerenkov light yield from 0.5 p.e./GeV to 1.2 p.e./GeV, as determined from the improved resolution for electron showers in the central tower. The width of the Q/S distributions for hadron showers improved accordingly, as illustrated by the black triangles in Figure 5. By increasing the light yield in this way, we effectively extended the energy test range of the original instrument. The fact that the experimental data obtained in this new configuration continued to scale with $[\sqrt{E}]^{-1}$, *i.e.* the fact that also the dash-dotted line in Figure 5 extrapolates to the bottom right corner of the plot, means that the limits of our method to improve the energy resolution by combining Čerenkov and dE/dx information are located beyond this extended reach as well.

However, we did find that the underlying relationship between the signals from the quartz fibers and the scintillating fibers did not change significantly over the energy range accessible in these studies. This relationship was determined by subdividing the $(Q + S)$ spectrum into narrow bins. For each bin, which is represented by a strip oriented perpendicular to the $Q/S = 1$ line in Figure 3a, we determined the average value of the signal from the scintillating fibers. These average values formed the "underlying banana curve", which gives a precise relationship between the Q/S signal ratio and the fraction of the energy deposited in this calorimeter. This relationship is shown in Figure 6.

This figure shows that the sensitivity and reliability of this method increases as a larger fraction of the shower energy is deposited in the calorimeter. This is no surprise. If an incoming hadron interacts in the calorimeter and produces few or no energetic π^0s, the resulting signals are not very dependent on the energy of the incoming particle, since most of the reaction products escape from the detector. It is, in that case, not well possible to make an accurate estimate of the energy of the incoming particle on the basis of the calorimeter signals. One could, for example, find on the basis of the Q/S ratio that $90 \pm 10\%$ of the shower energy escaped detection. However, that would only set a lower limit to the energy of the showering particle. If, on the other hand, a considerable fraction of the energy of the incoming hadron is converted into π^0s, the Q/S method might lead to quite accurate measurements of the shower leakage.

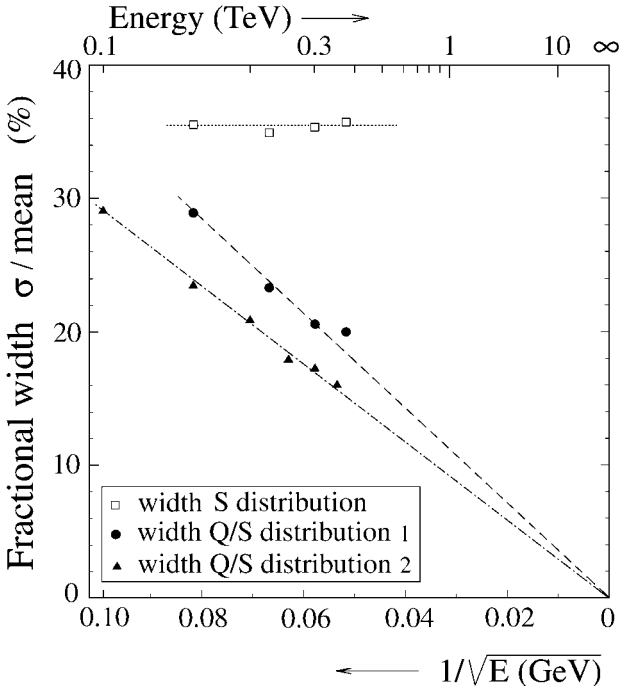

Figure 5: The fractional width of the distributions of the signals from the scintillating fibers S) and of the ratio of the signals from the quartz and the scintillating fibers (Q/S) as a function of the energy. The latter width is given for the original calorimeter configuration (1, black dots) and for a configuration with an increased amount of quartz (2, black triangles).

Consider, for example, a showering 10 TeV hadron that deposits roughly half of its energy in our calorimeter. The quartz signals would in that case consist of 2000–3000 photoelectrons. The experimental uncertainty on the Q/S signal ratio would thus be $\sim 2\%$ for this event. If photoelectron statistics were still the limiting factor at this energy, Figure 6 implies that our method would make it possible to determine the energy of the showering particle with a precision of $\sim 10\%$.

4 Conclusions

We have tested a hadron calorimeter that is based on the novel concept of measuring the properties of the developing showers with two different active media that provide complementary information about the showering particles. By measuring both the scintillation light and the Čerenkov light generated in hadron-induced showers, the energy containment in this very thin detector could be estimated event-by-event. Since fluctuations in the energy containment dominate the performance of this device, this information made it possible to improve the response function, both in terms of energy resolution and in terms of shape, by eliminating non-Gaussian tails.

A crucial parameter in this context turned out to be the ratio of the signals from the two types of fibers, Q/S. Events in which a large fraction of the energy of the incoming particle was spent on π^0 production, and which were thus well contained in the calorimeter, were characterized by a large Q/S value, whereas a small Q/S ratio was indicative for relatively large shower leakage.

We have shown that the beneficial effects of our method were limited by the small light yield of the quartz fibers. We have also shown that the underlying relationship between the signals from both types of fibers, which is responsible

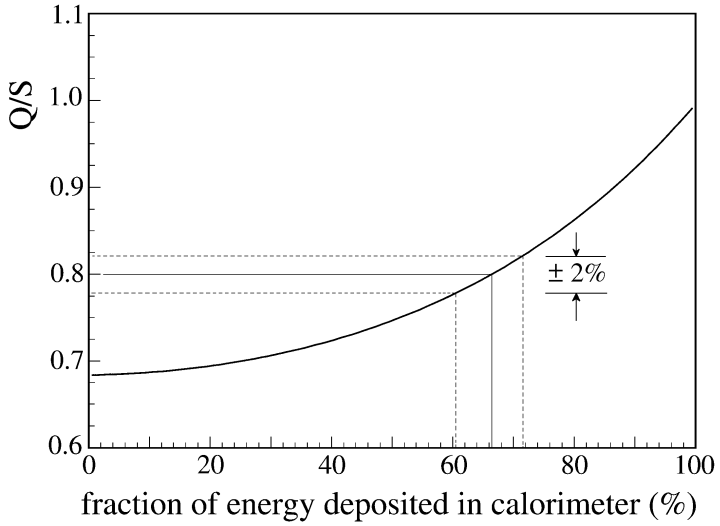

Figure 6: The relationship between the quartz/scintillator signal ratio and the fraction of the hadron energy deposited in the calorimeter.

for the beneficial effects of our method, is independent of energy, at least in the energy range accessible in our test beam experiments. Should this trend continue at higher energies, very substantial benefits of our method may be expected in the multi-TeV energy range for which this device is intended.

Coming back to the needs of limited-mass cosmic ray experiments outside the Earth's atmosphere, we would like to point again to Figure 5. This figure also shows the energy dependence of the hadronic energy resolution measured with the scintillating fibers *alone* (the open squares). This resolution is essentially independent of energy, which illustrates the fact that the light yield of the scintillating fibers is by no means a determining or limiting factor for this resolution. Since the hadronic resolution is completely dominated by fluctuations in shower leakage, a sampling calorimeter with a sampling fraction of less than 0.3% such as this one is thus as good (or bad) for hadron detection as a detector consisting of homogeneously sensitive scintillator material (*e.g.*, bismuth germanium oxide) with the same depth. Only by addressing the fluctuations that *dominate* the resolution, *i.e.* the fluctuations in shower containment, can one hope to improve this performance, as illustrated by the results presented in this paper.

References

[1] N. Akchurin *et al.* , Nucl. Instr. and Meth. **A399** (1997) 202.

[2] R. Wigmans, *Calorimetry – Energy Measurement in Particle Physics*, International Series of Monographs on Physics, Volume 107, Oxford University Press, Oxford (2000).

[3] G. Anzivino *et al.* , Nucl. Instr. and Meth. **A360** (1995) 237.

[4] O. Ganel and R. Wigmans, Nucl. Instr. and Meth. **A365** (1995) 104.